A&A 443, 769–775 (2005)
DOI: 10.1051/0004-6361:20053525

Astronomy & Astrophysics

Space weathering of near-Earth and main belt silicate-rich asteroids: observations and ion irradiation experiments

S. Marchi[1], R. Brunetto[2,3], S. Magrin[1], M. Lazzarin[1], and D. Gandolfi[4]

[1] Dipartimento di Astronomia, Vicolo dell'Osservatorio 2, 35122 Padova, Italy
e-mail: [marchi;s.magrin;lazzarin]@pd.astro.it
[2] Dipartimento di Fisica, Università di Lecce, via Arnesano, 73100 Lecce, Italy
e-mail: rbrunetto@ct.astro.it
[3] INAF - Osservatorio Astrofisico di Catania, via S. Sofia 78, 95123 Catania, Italy
[4] Dipartimento di Fisica e Astronomia, Università di Catania, via S. Sofia 78, 95123 Catania, Italy
e-mail: dgandolfi@ct.astro.it

Received 26 May 2005 / Accepted 29 July 2005

ABSTRACT

In this paper we report the results of a comparison between ion irradiation experiments (N^+, Ar^+, Ar^{++}) on silicates, a large spectral data set of silicate-rich (S-type) asteroids, and ordinary chondrite meteorites (OCs). Ion irradiation experiments – conducted on Fe-poor olivine, Fe-poor orthopyroxene, bulk silicate-rich rocks and one OC – have been monitored by means of reflectance spectroscopy (0.3–2.5 μm). All these experiments produce reddening and darkening of reflectance spectra. The observational data consist of a set of visible and near-infrared (0.4–2.4 μm) spectra of S-type asteroids, that belong to main belt (MBAs) and near-Earth (NEOs) populations. By analyzing the spectra of OCs, MBAs, and NEOs, we find a similar mineralogy between most asteroids and meteorites, but different distributions of spectral slopes. We interpret these findings in the frame of space weathering induced by solar wind ion irradiation.

Key words. minor planets, asteroids – meteors, meteoroids

1. Introduction

It is now widely accepted that the space environment alters the optical properties of airless bodies' surfaces. A number of physical processes have been proposed as relevant in this context (e.g. micrometeoroid impacts, solar wind bombardment, etc.). The result of all these effects on airless bodies is known as "space weathering".

Space weathering effects were initially studied on lunar soils; indeed it was found that the lunar soils returned from Apollo missions had optical properties that differed significantly from those of pristine lunar rocks (Conel & Nash 1970). The presence of iron particle coatings on lunar soils was suggested by Cassidy & Hapke (1975); these coatings should be produced by deposition of atoms sputtered by solar wind particles and deposition of gaseous species produced by micro-meteoritic impacts. More recently, Pieters et al. (2000) analyzed the products of space weathering of lunar soils, showing that nanophase reduced iron is produced on the surface of grains by a combination of vapor deposition and irradiation effects.

Since the '80s, space weathering effects were suggested as also present on other bodies, like asteroids, as well as on planets, like Mercury (see the detailed review by Chapman 2004). This idea was due to a mismatch between laboratory spectra of freshly-cut ordinary chondrites (OCs) and remote sensing spectra of S-type asteroids, which were thought to represent their parent bodies.

Recently, thanks to an increasing number of high quality asteroid spectra, along with dedicated laboratory experiments, new insights have arisen. The importance of laboratory experiments to simulate space weathering processes on asteroid-like materials is widely established. Experiments have been performed simulating solar wind and cosmic ion irradiation by keV–MeV ion irradiation, and assuming that micro-meteorite bombardment can be simulated by laser ablation.

The first experiments simulating space weathering of OCs were performed by Moroz et al. (1996), who used micro-pulsed laser irradiation; and the effect was to redden and darken reflectance spectra and also to produce a shift in the peak position of the 1 μm absorption band. Other laser ablation experiments were performed by Yamada et al. (1999) and Sasaki et al. (2001), who assumed that micrometeoroid impacts could be simulated by using a nanosecond pulsed Nd-YAG laser (1064 nm) on pellets of pressed silicate powder. Such experiments showed progressive (with increasing shots number) darkening and reddening of the UV-Vis-NIR silicate spectra.

They attributed the observed spectral weathering to formation of coating enriched in vapor-deposited nanophase iron (Sasaki et al. 2001).

On the other hand, low energy (keV) light ions (H^+ and He^+) (Dukes et al. 1999; Hapke 2001), and high energy (MeV) proton implantation (Yamada et al. 1999) produced only small changes in the spectra. A different result was obtained by Strazzulla et al. (2005), who performed ion irradiation of ordinary chondrite Epinal (H5) with Ar^{++} 60 keV, which produced strong darkening and reddening of the Vis-NIR spectra. Moreover, Brunetto & Strazzulla (2005) performed ion irradiation experiments of bulk silicates, using different ions (H^+, He^+, Ar^+, Ar^{++}) with different energies (60–400 keV). They find an increase in the 1 μm band spectral slope, which turned out to be strongly related to the number of displacements caused by colliding ions inside the sample, i.e. the elastic collisions with the target nuclei. A plausible explanation of the discrepancy between previous experiments and ours is that irradiation effects are much more efficient with high mass ions than low mass ones (see discussion in Brunetto & Strazzulla 2005).

One point to be underlined is that solar wind irradiation can redden reflectance spectra by two processes: creation of displacements (Brunetto & Strazzulla 2005) and sputtering of iron from silicates and the deposition of submicroscopic metallic iron on adjacent grains (e.g. see Clark et al. 2002). Atom displacements occur along the whole ion track, up to a depth about equal to the ion mean penetration depth R_p, so the displacement of atoms is a volume effect. In particular, when the displacements occur near the target surface, some atoms can leave the target; i.e. sputtering can occur. Consequently, sputtering is essentially a surface effect. Sputtering and displacement processes occur simultaneously; nevertheless, a relatively low fluence (10^{15}–10^{16} ions/cm^2) is enough to cause strong damage up to a depth of R_p, while at these fluences the amount of sputtered material is negligible (of the order of monolayer).

In this paper we report the results of a comparison between ion irradiation experiments on silicates, a large data set of silicate-rich asteroid, and meteorites spectra.

2. Observational data

The observational data used in this work consist of a large set of visible and near-infrared spectra of silicate-rich (generally indicated by S-type) asteroids. The vast majority of these objects are in the main belt (MB). However a significant number of S-types have also been detected in near-Earth space thanks to recent surveys, like SINEO (Lazzarin et al. 2005, 2004). This latter source of S-types is also of greater interest because of its direct connection with meteorites and because, owing to their closeness, it permits study of smaller bodies. In the present work, we consider only objects for which the whole 0.4–2.4 μm range is available, because we are interested in a detailed analysis of the diagnostic 1 μm and 2 μm absorption bands due to olivine and pyroxene. Moreover, we compare asteroid data with a large number of meteorite spectra from RELAB (`http://www.planetary.brown.edu/relab/`). In the following we report a detailed description of the data used.

Main Belt asteroids. The NIR spectra of MBAs have been retrieved from the 52-color survey (Bell et al. 1985) and SMASSIR (Burbine 2000). As they cover the range 0.9–2.4 μm, we extended them in the visible by using the data from SMASSI (Xu 1994) and SMASSII (Bus 1999). Spectra have been joined by minimizing the RMS of the differences in the overlapping region. Notice that for some asteroids the range 0.9–1.6 μm was present in both the 52-color and SMASSIR. In this case we privileged the spectral data instead of the photometric ones. A detailed description of the data used is provided in Table 1.

Near-Earth objects. Most parts of these data come from our SINEO survey, as it is the only existing NEO survey up to 2.5 μm available so far. It consists of more than 100 spectra, 24 of which belong to the S-complex and have the full 0.4–2.5 μm coverage. Only few spectra come from Binzel et al. (2004a) and from Rivkin et al. (2004). Another 3 spectra were obtained joining data from Binzel et al. (2004b) and from the 52-color survey. A list containing all NEOs considered in this paper can be found in Table 2.

Meteorites. We retrieved a large number of meteorites spectra from RELAB. Details of the materials used are provided in Table 3. All the meteorites selected belong to the ordinary chondrite group, because OCs have been suggested as representing the best analogues of S-type asteroids by several authors (see for example Gaffey et al. 1993). As in our work we deal with space weathering, we considered only those meteorites for whose no trace of alteration was reported. For this reason all the spectra indicating some natural alteration process (in the headers or in the description file) were discarded. Also those altered in laboratory (e.g. laser irradiated, washed etc.) were not considered.

All the spectra were analyzed in terms of the spectral parametrization developed by Gaffey et al. (1993). For each spectrum, we computed the slope of continuum across the 1 μm absorption band, the 1 μm band (BI) and 2 μm band (BII) area, and BI depth and peak position. The slope thus defined is representative of spectral reddening. We want to point out that by this analysis the BII/BI area ratio and the BI peak position are representative of the composition and that the slope is highly representative of space weathering alteration (see Strazzulla et al. 2005; Hiroi & Sasaki 2001). However, we should keep in mind that this analysis is not able to constrain the presence of featureless compounds, like metals and glasses. Nevertheless, it remains a good way to describe the silicate-rich bodies which are thought to be mostly made of olivine and pyroxene.

3. Experimental data

Ion irradiation experiments were performed in the Laboratory of Experimental Astrophysics in Catania, using different ions (N^+, Ar^+, Ar^{++}) and energies. The outcomes were monitored by means of reflectance spectroscopy (0.3–2.5 μm). Here we present new experiments simulating space weathering by solar wind ions by ion irradiation experiments (200 keV) of Fe-poor olivine (from Bamble, Norway) and of Fe–poor orthopyroxene (from San Carlos, Arizona, USA), and irradiation of bulk silicate-rich rocks (Eifel silicate, from Germany).

Table 1. List of Main Belt asteroids considered in the present work. Column 2 indicates the origin of data used to obtain spectra in the entire range until 2.4 μm. s1: SMASSI data; s2: SMASSII data; sIR: SMASSIR data; 52c: 52-color data (see text for details).

Number	Reference	Spectral range	Slope	λ_{BI}	BII/BI
3	s2+sIR+52c	0.44–2.46	0.164	0.940	0.512
5	s2+sIR+52c	0.44–2.46	0.256	0.910	0.568
6	s2+sIR+52c	0.44–2.51	0.248	0.930	0.475
7	s2+sIR+52c	0.44–2.56	0.332	0.940	0.268
11	s2+sIR+52c	0.44–2.56	0.262	0.980	0.385
12	s2+sIR+52c	0.44–2.46	0.274	1.140	0.196
15	s2+sIR+52c	0.44–2.41	0.227	1.000	0.137
18	s2+sIR+52c	0.44–2.56	0.309	0.900	0.340
20	s2+sIR+52c	0.44–2.51	0.164	0.920	0.967
25	s2+sIR+52c	0.44–2.56	0.513	0.952	0.294
26	s2+sIR+52c	0.44–2.46	0.209	0.974	0.226
27	s2+52c	0.44–2.51	0.237	0.960	0.473
29	s2+sIR+52c	0.44–2.56	0.216	0.980	0.623
32	s2+sIR+52c	0.44–2.41	0.206	0.910	0.263
33	s2+sIR+52c	0.44–2.56	0.164	0.910	0.674
37	s2+sIR+52c	0.44–2.51	0.400	0.910	0.947
39	s2+sIR+52c	0.44–2.46	0.147	1.050	0.345
40	s2+sIR+52c	0.44–2.56	0.148	0.930	0.401
42	s2+sIR+52c	0.44–2.56	0.241	1.060	0.009
43	s2+sIR+52c	0.44–2.56	0.324	0.980	0.291
57	s2+sIR+52c	0.44–2.51	0.342	0.920	0.892
63	s2+sIR+52c	0.44–2.51	0.539	0.930	0.376
67	s2+52c	0.44–2.46	0.176	0.930	0.574
68	s1+sIR+52c	0.47–2.56	0.263	1.040	0.209
80	s2+sIR+52c	0.44–2.51	0.410	0.940	0.231
82	s2+sIR+52c	0.44–2.46	0.027	0.910	1.108
89	s2+52c	0.44–2.46	0.274	1.030	0.364
101	s2+52c	0.44–2.51	0.181	0.930	0.748
103	s2+52c	0.44–2.51	0.167	0.930	0.433
113	s2+sIR+52c	0.44–2.46	0.256	1.020	0.026
115	s2+52c	0.44–2.56	0.254	0.950	0.393
116	s2+52c	0.44–2.56	0.185	0.890	0.657
138	s1+52c	0.49–2.51	0.209	1.010	0.090
152	s2+52c	0.44–2.51	0.279	0.920	0.934
218	s1+52c	0.47–2.56	0.249	0.980	0.908
246	s2+sIR+52c	0.44–2.56	0.555	1.100	0.247
258	s2+52c	0.44–2.46	0.165	0.910	0.709
264	s2+52c	0.44–2.51	0.181	0.930	0.374
289	s2+sIR+52c	0.44–2.46	0.882	1.100	0.007
346	s2+sIR+52c	0.44–2.56	0.346	0.950	0.327
349	s2+sIR+52c	0.44–2.51	0.472	0.940	0.696
354	s2+sIR+52c	0.44–2.46	0.594	1.080	0.033
376	s2+52c	0.44–2.46	0.349	0.960	0.468
387	s2+52c	0.44–2.51	0.179	1.050	3.992
389	s2+sIR+52c	0.44–2.41	0.219	0.900	0.619
446	s2+sIR+52c	0.44–2.41	0.826	1.090	0.055
532	s2+52c	0.44–2.41	0.265	0.960	0.158
584	s2+sIR+52c	0.44–2.51	0.571	0.970	0.433
653	s2+sIR+52c	0.44–2.46	–0.082	1.060	0.825
674	s2+52c	0.44–2.41	0.177	0.910	0.830
863	s2+sIR+52c	0.44–2.41	1.118	1.090	0.060
980	s2+sIR+52c	0.44–2.51	0.109	1.000	0.389

Pellets of olivine and orhopyroxene were obtained by pressing their powders with grain sizes of about 100–200 μm. Our Eifel silicates consisted of freshly cut samples from rock fragments, with a surface roughness of about 100 μm. For better comparison with asteroid spectra we also considered irradiation of Epinal meteorite and of other bulk silicate-rich rocks (Jackson silicate), which have already been presented in Strazzulla et al. (2005) and Brunetto & Strazzulla (2005).

Table 2. List of Near Earth asteroids considered. Column 2 indicates the source of data. sineo: SINEO project; sm6, sm8, and sm9: NEOs within SMASS survey (respectively: Binzel et al. 2004a,b; Rivkin et al. 2004); 52c: 52-color data (see text for details).

Number	Name	Reference	Spectral range	Slope	λ_{BI}	BII/BI
719	Albert	sineo	0.40–2.45	0.320	0.951	0.276
3102	Krok	sineo	0.40–2.45	0.213	0.961	0.152
3753	Cruithne	sineo	0.40–2.54	0.219	0.950	0.264
4587	Rees	sineo	0.50–2.48	0.213	0.909	0.455
6489	Golevka	sineo	0.40–2.54	0.252	0.956	0.403
7341	1991 VK	sineo	0.40–2.51	0.268	0.969	0.428
8013	Gordonmoore	sineo	0.49–2.45	0.013	0.975	0.073
11054	1991 FA	sineo	0.40–2.50	0.667	0.961	0.079
35107	1991 VH	sineo	0.50–2.50	0.361	0.985	0.698
35396	1997 XF11	sineo	0.50–2.49	0.418	0.958	0.048
52340	1992 SY	sineo	0.50–2.50	0.072	1.021	1.020
54071	2000 GQ146	sineo	0.40–2.50	0.390	0.999	0.264
66251	1999 GJ2	sineo	0.50–2.49	0.603	0.949	0.364
68346	2001 KZ66	sineo	0.50–2.46	0.245	0.974	0.100
88710	2001 SL9	sineo	0.40–2.48	0.317	0.918	1.786
98943	2001 CC21	sineo	0.50–2.50	0.445	0.956	0.089
	2000 EZ148	sineo	0.40–2.48	0.026	0.963	0.340
	2002 AL14	sineo	0.50–2.47	0.705	0.971	0.504
	2002 QE15	sineo	0.50–2.49	0.601	0.968	0.336
	2002 TD60	sineo	0.50–2.50	0.527	0.937	0.235
	2002 TP69	sineo	0.50–2.49	0.235	0.950	1.252
	2002 VP69	sineo	0.40–2.50	0.267	0.991	0.252
	2002 YB12	sineo	0.50–2.49	0.187	0.938	0.097
	2003 KR18	sineo	0.50–2.47	0.306	0.969	0.214
433	Eros	sm9	0.44–2.49	0.333	0.970	0.318
1036	Ganymed	sm8+52c	0.44–2.51	0.344	0.920	0.737
1627	Ivar	sm8+52c	0.44–2.56	0.254	0.950	0.174
1685	Toro	sm6	0.44–2.43	0.202	0.970	0.441
1866	Sisyphus	sm8+52c	0.44–2.46	0.197	0.950	0.243
1943	Anteros	sm6	0.36–2.43	0.561	0.960	0.457
19356	1997 GH3	sm9	0.44–2.41	0.100	0.960	0.541

Table 3. Spectra acquired by different investigators with the NASA RELAB facility at Brown University. This table lists the number of RELAB OC meteorites used from different Principal Investigators.

PI code	PI full name	Spectra used
CMP	Carlé M. Pieters	85
DTB	Dan Britt	12
FPF	Fraser P. Fanale	25
JFB	Jeffery F. Bell	4
LAM	Lucy Ann McFadden	5
MJG	Michael J. Gaffey	39
TXH	Takahiro Hiroi	14
Total		184

The experimental set-up consisted of a stainless steel vacuum chamber ($P < 10^{-7}$ mbar), where the samples are in contact with a sample holder, held in place by a metal corona ring, and the sample holder is in thermal contact with the chamber, which is maintained at room temperature. The vacuum chamber is interfaced to an ion implanter (Danfysik 1080–200) from which ions with energy from 30 keV up to 200 keV (400 keV for double ionization) can be obtained. Hemispherical reflectance spectra have been acquired using a UV-Vis-NIR spectrometer (Perkin Elmer, Lamba 19). A $BaSO_4$ substrate is used as reference material in the 0.3–2.5 μm spectral range. Further experimental details can be found elsewhere (Brunetto & Strazzulla 2005).

The ion mean penetration depth (R_p), the stopping power (energy deposited per unit path length), and the amount of elastic versus inelastic energy loss are functions of the ion energy and mass and of the properties of the target. When ion irradiation experiments are performed to simulate solar wind and cosmic ion irradiation, the corresponding type of ion can be easily obtained in laboratory, though it is more difficult to reproduce the energy distribution of these ions. Therefore, the laboratory results can be used for astrophysical application only when we find out which is the physical mechanism that is causing the observed effects, i.e. when we can extrapolate the laboratory data to a wider range of ion masses and energies. Brunetto & Strazzulla (2005) have found that the physical mechanism that is responsible for the weathering effects is the energy lost by elastic collisions between ions and target nuclei, and the damage parameter d (namely number of displacements/cm^2) can be used to compare the effects of different ions and energies. This means that ion irradiation experiments can be considered a direct reproduction of solar wind irradiation effects, and we can apply our simulations to space weathering of MBAs and NEOs. We consequently calculated the damage parameters (number

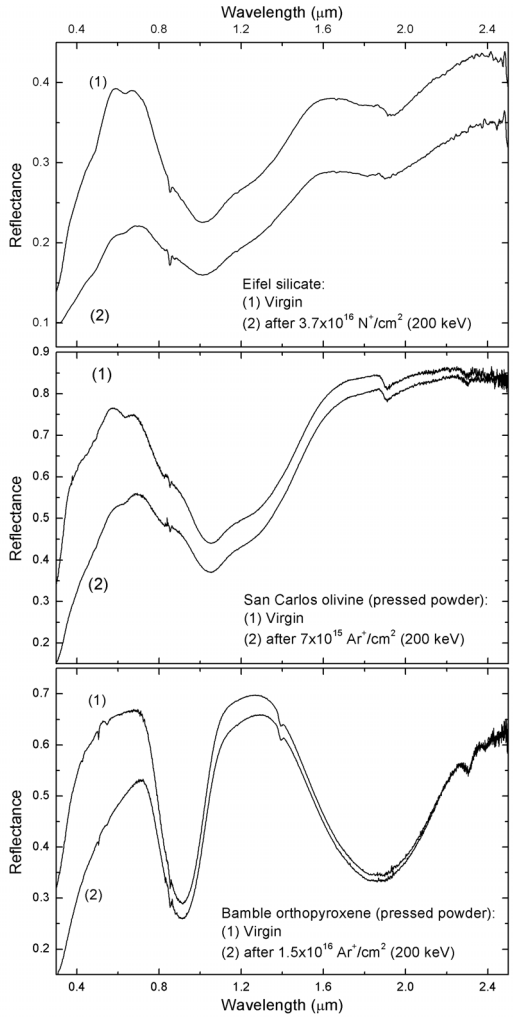

Fig. 1. Reflectance spectra of virgin and irradiated Eifel (*upper panel*), San Carlos orthopyroxene (*middle panel*), and Bamble olivine (*lower panel*).

of displacements per ion, stopping power, and mean penetration depth) for our experiments, by using the SRIM simulation code (at `http://www.SRIM.org/`; Ziegler et al. 1985).

4. Results

Bulk Eifel silicate rocks are rich in olivine, and have a small content of pyroxene, as can be seen in Fig. 1 (upper panel). Indeed, the spectrum of unirradiated Eifel sample exhibits a very strong and broad band at about 1 μm (BI), which is due to the presence of ferrous iron Fe^{2+} in olivine crystals but is also present in pyroxene. It is also evident a less intense broad 2 μm band (BII) that is characteristic of pyroxene but not olivine. We irradiated the Eifel sample with 3.7×10^{16} N^+/cm^2 (energy of 200 keV, $d = 3.07 \times 10^{19}$ displ/cm^2, and $R_p = 360 \pm 100$ nm). The spectrum of irradiated Eifel (upper panel of Fig. 1) shows strong darkening and reddening, and weathering effects are strong in the whole observed spectral range. The area of BI is reduced as the slope of the continuum across BI increases, and a similar effect is observed for BII.

The reflectance spectra of San Carlos olivine and Bamble orthopyroxene are plotted in Fig. 1 (middle and lower panel). They were irradiated with 7×10^{15} Ar^+/cm^2 and 1.5×10^{16} Ar^+/cm^2 (energy of 200 keV, and $R_p = 160 \pm 60$ nm) corresponding to $d = 1.4 \times 10^{19}$ and 3×10^{19} displ/cm^2, respectively (see Fig. 1). Also in these cases, darkening and reddening of reflectance spectra are apparent.

This spectral reddening agrees with the results of previous experiments of ion irradiation of the OC Epinal meteorite (Strazzulla et al. 2005) and of Jackson silicates (Brunetto & Strazzulla 2005). Furthermore, we note that the weathering process is active both on bulk samples and pressed powder samples.

Notice that the thickness of the damaged region at these energies is lower than 1 μm; i.e. the reddening and darkening process of reflectance spectra is due to displacements in the very upper layers of the target. A similar effect of upper layer alteration should be present in asteroids, which would cause the mismatch between the slope of asteroids and that of OCs.

In this respect, one result concerns the well-known lack of OCs analogues (which represent the largest number of falls on Earth) among minor bodies. The situation is shown in Fig. 2, where the slope distributions of OCs, NEOs, and MBAs are very different. Some authors (e.g. see Lazzarin et al. 1997; Binzel et al. 1996) report the occurrence of OC-like bodies among small asteroids (and in particular among NEOs). Indeed the blue tail of MBAs and NEOs distributions overlap the OCs distribution. However, in terms of numbers, these findings still represent only some exceptions.

Nevertheless, OCs distribution (representative of pristine materials) peaks at slope ∼0, and is by far less red than the NEOs and MBAs distributions. On the contrary, the two latter distributions are basically indistinguishable. The striking feature is that, if we define the limiting slope below which 95% of the OCs lie (corresponding to a slope of $S_w = 0.138$ μm^{-1}), we find that 83% of the NEOs and 94% of the MBAs are redder than S_w. Thus only 17% of NEOs and 6% of MBAs are compatible with OCs spectra. Although these percentages can be affected by low number statistic, the NEO population seems to contain a higher percentage of OC-like objects. In this respect, the S_w value can be regarded as an indicator of space weathering: objects redder than S_w may be considered – with high confidence – as weathered, while, in terms of slope, objects below S_w are fully compatible with OCs. We also underline that, in spite of the wide size-range involved, NEOs and MBAs span a similar interval of slopes and that the asteroid slope distributions have a broader FWHM with respect to that of OCs (of roughly a factor of 3). A possible explanation for the different FWHM between the asteroid and OCs slope distributions could be that asteroids spend different exposure times in weathering environment, also suffering resurfacing processes.

Figure 2 also reports the results for ion irradiation experiments. Epinal shows the trend for a typical OC, while Jackson is representative of the maximum reddening attained in laboratory experiments, which largely overcome asteroid slopes. Therefore the shift between OCs and asteroids distributions can be explained by ion irradiation experiments.

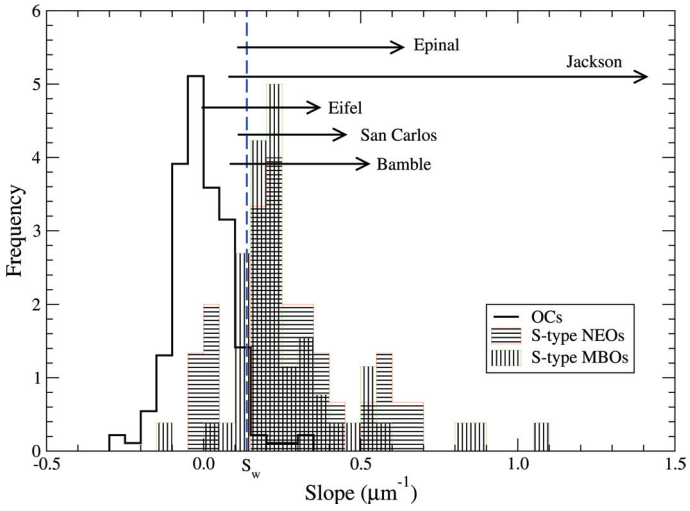

Fig. 2. Spectral slope distributions of OCs, NEOs, and MBAs. Each distribution has been normalized (area = 1). The vertical dashed line marks the 95% OCs limit (corresponding to a slope of $S_w = 0.138\ \mu m^{-1}$). Horizontal arrows mark the reddening measured for irradiated Epinal, Jackson (from Strazzulla et al. 2005; and Brunetto & Strazzulla 2005), Eifel, San Carlos, and Bamble (this work).

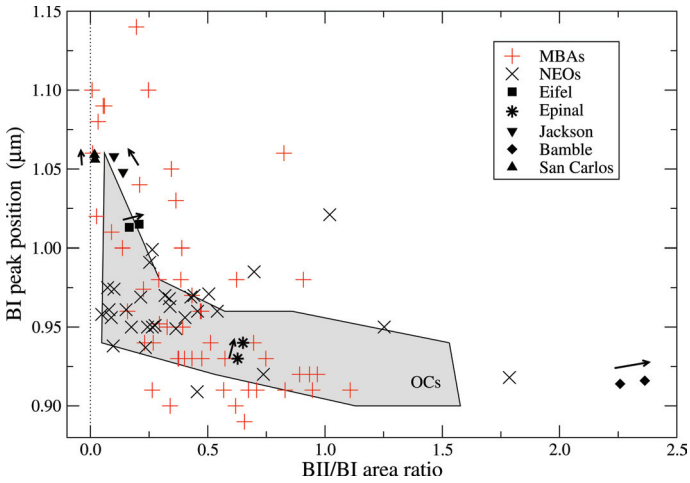

Fig. 3. Band I peak position vs. BII/BI area ratio for MBAs and NEOs. Positions for virgin and irradiated silicate are also shown (arrows show their trend from virgin to irradiated). The shaded area corresponds to the region occupied by OCs. Symbol dimensions correspond to maximum error bars.

Figure 3 shows the BI peak position as a function of the BII/BI area ratio. From this plot it is possible to get information about the mineralogy of the analyzed bodies. Gaffey et al. (1993) used a similar plot to separate the S-type asteroids into seven classes (from SI to SVII), where the SIV class had been defined from the corresponding mineralogy of OCs. We enlarged the statistic of both asteroids and OCs, so that from Fig. 3 we can deduce that the SIV class is indeed much wider than that defined by Gaffey et al. (1993). A second point that arises from Fig. 3 is that irradiation does not change the BII/BI area ratio significantly.

A further important result concerns the suitability of using of the slope parameter to study the effects of space weathering. In Fig. 4 we show the spectral slope as a function of the BII/BI area ratio, for MBAs, NEOs, OCs, and laboratory experiments. It turns out that space weathering acts mainly on the slope, but only marginally on the ratio BII/BI, for both pressed powder (San Carlos and Bamble) and bulk samples (Jackson, Eifel, Epinal). On the other hand, the ratio BII/BI is representative of the composition. Thus, the discrepancy between meteorites and asteroids has mainly to be ascribed to the spectral slope, and this process is reproduced well by our ion irradiation experiments.

Another interesting issue related to Fig. 4 is that MBAs (and NEOs) have a triangle-shaped distribution, with the highest slopes achieved for low values of BII/BI, namely for high olivine contents. This seems to be in agreement with our experimental data: San Carlos olivine reddens more efficiently than Bamble orthopyroxene. Indeed, both reach a similar spectral slope of about 0.5 μm^{-1}, but their damage values are about 1.4×10^{19} displ/cm^2 and 3×10^{19} displ/cm^2, respectively. However, this point deserves more dedicated experiments in order to be confirmed, and will be the subject of further investigations.

From the spectra of irradiated Epinal, Strazzulla et al. (2005) have estimated a reddening time-scale of about 10^5 years at 1 AU (Astronomical Unit) from the Sun. The results reported here indicate that most of the spectral slopes of asteroids can be reproduced by damage values in the range $1-3 \times 10^{19}$ displ/cm^2 (see Fig. 4) , in agreement with what has been calculated for Epinal (Brunetto & Strazzulla 2005). We, therefore, confirm that ion irradiation is a very efficient weathering process. Nevertheless, this is only one of the processes that can affect asteroid surfaces; in particular, the time-scale of ion-induced reddening is not expected to strictly correspond to the lifetime of the asteroid surfaces, as several rejuvenating

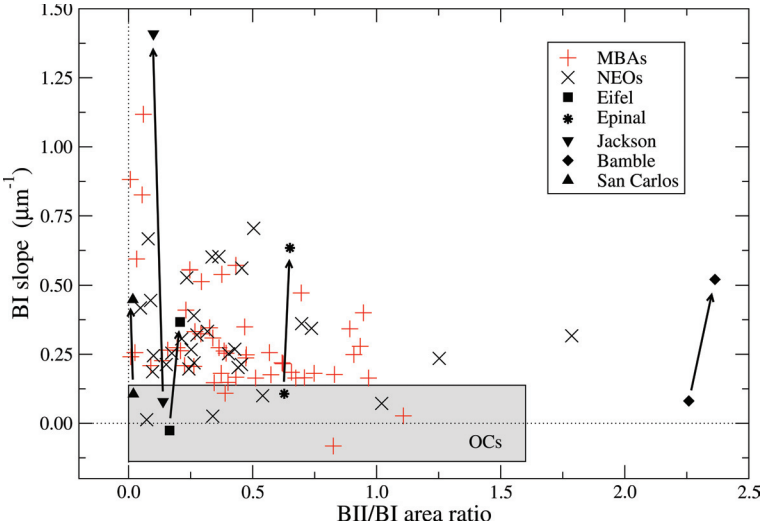

Fig. 4. Spectral slope vs. BII/BI area ratio for MBAs and NEOs. Vertical arrows show the trend from virgin to irradiated silicates. The shaded box contains 95% of OCs as described in Fig. 2. Symbol dimensions correspond to maximum error bars.

mechanism can be present, whose efficiency could be able to partially compensate for the reddening induced by solar wind ions. Moreover, at the MB distance to the Sun, other mechanisms – such as micrometeorite impacts – could also be as efficient as ion bombardment for the weathering.

5. Summary

We have compared a wide set of asteroid and meteorite spectra with ion irradiation experiments. From the results of this comparison, some points can be established:

- OCs and S-type asteroids exhibit a similar mineralogy, as deduced from band parameters, more than what was previously assumed. Nevertheless, a significant mismatch was observed in the Vis-NIR spectra, which is due to very different distributions of spectral slope.
- The continuum slope above BI band is a good parameter to quantify the degree of space weathering. Thus, we define a 95% OC slope limit (S_w) beyond which an asteroid can be considered as "weathered". We find that about 83% and 94% of the observed NEOs and MBAs, respectively, have a higher slope than this limit. Moreover, asteroid slope distributions exhibit a noticeably broader FWHM with respect to OCs distribution of about a factor of 3.
- Ion irradiation can explain the shift of the OC distribution toward asteroid distributions. Spectra of unaltered and irradiated silicates have slopes that span a wider range than that observed in NEOs and MBAs.
- MBA and NEO slope distributions do not differ significantly from each other. However, if compared with OCs, they exhibit an asymmetrical slope distribution, possibly due to a different rate of weathering between olivine-rich asteroids and pyroxene-rich ones, a behavior that will be a subject of further investigations.

Acknowledgements. We thank G. Strazzulla for his helpful comments, and G. A. Baratta and F. Spinella for their help during the experiments. We also thank V. Orofino for providing us with the silicate samples. Authors thank the anonymous referee who helped to improve the paper by means of useful comments.

References

Bell, J. F., Hawke, B. R., Owensby, P. D., & Gaffey, M. J. 1985, BAAS 17, 729
Binzel, R. P., Bus, S. J., Burbine, T. H., & Sunshine, J. M. 1996, Science, 273, 946
Binzel, R. P., Birlan, M., Bus, S. J., et al. 2004a, Planetary and Space Science, 52, 291
Binzel, R. P., Rivkin, A. S., Stuart, J. S., et al. 2004b, Icarus, 170, 259
Burbine, T. H. 2000, Ph.D. Thesis, Massachusetts Institute of Technology
Bus, S. J. 1999, Ph.D. Thesis, Massachusetts Institute of Technology
Brunetto, R., & Strazzulla, G. 2005, Icarus, in press
Cassidy, W., & Hapke, B. 1975, Icarus, 25, 371
Chapman, C. R. 2004, AREPS, 32, 539
Clark, B. E., Hapke, B., Pieters, C., & Britt, D. 2002, Asteroids III, ed. W. F. Bottke Jr., A. Cellino, P. Paolicchi, & R. P. Binzel (Tucson: University of Arizona Press), 585
Conel, J. E., & Nash, D. B. 1970, Geochim. Cosmochim. Acta Suppl., 1, 2013
Dukes, C. A., Baragiola, R. A., & McFadden, L. A. 1999, J. Geophys. Res., 104, 1865
Gaffey, M. J., Burbine, T. H., Piatek, J. L., et al. 1993, Icarus, 106, 573
Hapke, B. 2001, J. Geophys. Res., 106, E5, 10,039
Hiroi, T., & Sasaki, S. 2001, Meteorit. Planet. Sci., 36, 1587
Lazzarin, M., di Martino, M., Barucci, M. A., Doressoundiram, A., & Florczak, M. 1997, A&A, 327, 388
Lazzarin, M., Marchi, S., Barucci, M. A., Di Martino, M., & Barbieri, C. 2004, Icarus, 169, 373
Lazzarin, M., Marchi, S., Magrin, S., & Licandro, J. 2005, MNRAS, 362, 1575
Moroz, L. V., Fisenko, A. V., Semjonova, L. F., Pieters, C. M., & Korotaeva, N. N. 1996, Icarus, 122, 366
Pieters, C. M., Taylor, L. A., Noble, S. K., et al. 2000, Meteorit. Planet. Sci., 35, 1101
Rivkin, A. S., Binzel, R. P., Sunshine, J., et al. 2004, Icarus, 172, 408
Sasaki, S., Nakamura, K., Hamabe, Y., Kurahashi, E., & Hiroi, T. 2001, Nature, 410, 555
Strazzulla, G., Dotto, E., Binzel, R., et al. 2005, Icarus, 174, 31
Xu, S. 1994, Ph.D. Thesis, Massachusetts Institute of Technology
Yamada, M., Sasaki, S., Nagahara, H., et al. 1999, Earth Planets Space 51, 1255
Ziegler, J. F., Biersack, J. P., & Littmark, U. 1985, The Stopping and Range of Ions in Solids (New York: Pergamon Press)